Graphical Evaluation of the Favorability of Adsorption Processes by Using Conditional Langmuir Constant

ARTICLE · JANUARY 2013

READS
47

1 AUTHOR:

Xian Xiang Sun
Changzhou University
14 PUBLICATIONS **154** CITATIONS

SEE PROFILE

I&EC research
Industrial & Engineering Chemistry Research

Article

pubs.acs.org/IECR

Graphical Evaluation of the Favorability of Adsorption Processes by Using Conditional Langmuir Constant

Cheng-Jun Sun,[†] Ling-Zhi Sun,*[,‡] and Xian-Xiang Sun[§]

[†]College of Materials and Textile Engineering, Jiaxing Univesity, Jiaxing 314001, China

[‡]Institute of Bioscience and Technology, Yancheng Teachers University, Yancheng 224051, China

[§]School of Petrochemical Engineering, Changzhou University, Changzhou 213164, China

Supporting Information

ABSTRACT: A graphical method for evaluating the Langmuir favorable adsorption is proposed in this work. The conditional Langmuir constant (K_L^N), a new parameter related to the Langmuir equilibrium constant (K_L), can be used to predict the shapes of Langmuir favorable adsorption isotherms. On the dimensionless Langmuir isotherm diagram, all the Langmuir favorable adsorptions ($0 < R_L < 1$) are further divided into three subgroups: favorable adsorption, very favorable adsorption, and highly favorable or pseudoirreversible adsorption, with two critical Langmuir constants (K_L^{N1} and K_L^{N2}) as the demarcation point. The feasibility of the method is demonstrated by analyzing 14 adsorption systems. The graphical method is effective and intuitional, and can be used for the favorable evaluation of any Langmuir isotherms. This method shows the advantage that the parameter K_L^N does not depend on the initial adsorbate concentration (c_o) over R_L method.

1. INTRODUCTION

Adsorption is a widely used separation technique for gas or liquid mixtures, and is successfully applied to purification processes, such as the treatment of aqueous pollution effluents,[1] the large volume gas stream purification and solvent enrichment,[2,3] preparative chromatographic processes, [4] and so forth. The equilibrium between adsorbed component and unadsorbed component can be represented by adsorption isotherm. This isotherm expresses the specific relation between the adsorbate concentration (i.e., the equilibrium concentration in aqueous solution) and the amount of adsorption on the adsorbent surface (i.e., the equilibrium concentration in solid phases) at constant temperature. Adsorption isotherms are critical to optimize the adsorption mechanism and adsorbents capacities, characterize the surface properties, and effectively design the adsorption systems.[5] Among the wide variety of equilibrium isotherm models, the Langmuir isotherm presented by Langmuir in 1918[6] is the simplest and the most useful isotherm for physical and chemical adsorption, i.e., many real sorption processes,[1] liquid-phase systems,[7−11] and some adsorption systems with carbon nanotubes[12−14] or nanotube composites[15] as adsorbents.

The essential characteristic of Langmuir isotherm can be characterized with separation factor, R_L, a dimensionless constant defined with the following equation:[16]

$$R_L = \frac{1}{1 + K_L c_0} \tag{1}$$

Here, K_L is the Langmuir constant related to the enthalpy of adsorption through the Van't Hoff equation, and c_o is the initial concentration of adsorbate. R_L indicates the type of isotherm: unfavorable ($R_L > 1$), linear ($R_L = 1$), favorable ($0 < R_L < 1$), or irreversible ($R_L = 0$). The evaluation methodology based on the magnitude of R_L value is termed the R_L method in this paper.

The evaluation of favorable adsorption plays an important role in optimizing an adsorbent and designing an adsorption process. The R_L method, in which the criterion of favorable adsorption is $0 < R_L < 1$, has been widely applied for many adsorption systems.[2,9−12]

In some cases, the favorability of an adsorption is also evaluated with the Freundlich's intensity factor n_F in the Freundlich isotherm.[17] The adsorption is generally classified with the values of n_F: good (2−10), moderately difficult (1−2), and poor (<1).[11] This method is denoted as the n_F method in this work. However, in some cases, this method is not always effective, e.g., when $n_F > 10$ or there are two different values of n_F. Some examples can be seen in section 5.2. A favorable parameter, $K_L c_o$, which is numerically equal to $(1/R_L) - 1$, recently was also used for the adsorption evaluation.[18,19] When $K_L c_o$ is in the range from 1 to 10, the adsorption system is termed as favorable. When its value is above 10, the isotherm is highly favorable.[19]

During the application of the R_L method, two problems need to be overcome. First, the variation of R_L resulting from different initial concentrations (c_o) affects the evaluating results. For instance, for the adsorption of methylene blue (MB) on Amberlite XAD-2, R_L (0.769) at c_o = 50 mg L^{-1} is over 10 times more than R_L (0.077) at c_o = 2000 mg L^{-1}.[10] Similarly, R_L (0.514) of fly ash adsorbent at a low concentration of Reactive Black 5(RB) was over 10 times more than R_L (0.050) at a high concentration.[9] Since there are no standard initial concentrations of adsorbate (c_o), it is sometimes difficult to evaluate the isotherms by comparing R_L at different initial concentrations. Second, the range of R_L (0−1) is so wide that a further

Received: May 17, 2013
Revised: August 21, 2013
Accepted: August 23, 2013
Published: August 23, 2013

approach is needed to identify several favorable subgroups,[18] which has been demonstrated in many practical examples.[18] Weber et al.[20] first evaluated two favorable adsorption isotherms with the terms of "favorable" (R_L = 0.364) and "very favorable" (R_L = 0.054), respectively.

The main purpose of this work is to present a graphical K_L^N method to evaluate the favorability of Langmuir adsorption isotherm on the dimensionless Langmuir isotherm diagram through the conditional Langmuir constant (K_L^N). K_L^N is also related to the equated maximum adsorption capacity (EMAC) and the maximum equilibrium concentration c_m.

In this paper, we demonstrate that K_L^N can be used to characterize the shapes of Langmuir adsorption isotherms with EMAC. The evaluation methodology of the graphical K_L^N method is also described. To demonstrate the applicability of this method, the favorability of three Propr·HCl/Propr-IP adsorption systems and 11 others in the literature are evaluated using the K_L^N method. The practical ranges of three evaluation methods, K_L^N, R_L, and n_F method, are also discussed.

2. THEORETICAL DEVELOPMENT

2.1. Shape of Langmuir Favorable Adsorption Isotherm and K_L^N. The Langmuir adsorption isotherm can be expressed by the following equation:

$$q_e = \frac{q_m K_L c_e}{1 + K_L c_e} \tag{2}$$

Here, q_e (mmol g^{-1}) is the equilibrium adsorption capacity of adsorbate, q_m (mmol.g^{-1}) is the maximum adsorption capacity when the adsorbent is covered with a monolayer, c_e (mM) is the equilibrium concentration of adsorbate in the bulk solution, and K_L (L $mmol^{-1}$) is the Langmuir adsorption constant. The values of q_m and K_L in the Langmuir model can be determined through the slope and the intercept of the plot of c_e/q_e versus c_e, or through fitting the parameters in the nonlinear equation (eq 2).

As mentioned before, because the Langmuir isotherm constant separation factor, R_L, indicates the shapes of the Langmuir adsorption isotherm curves, R_L can be used to characterize the favorability of the adsorption processes. According to eq 1, obviously, there are the following relationships: $K_L > 0$ when $R_L < 1$; $K_L = 0$ when $R_L = 1$, and $K_L < 0$ when $R_L > 1$. This suggests that K_L is also as effective as the factor R_L to graphically characterize the shape of Langmuir isotherm K_L, which has not been noticed for a long time. As shown in Figure 1, the isotherm curve is initially convex to the concentration axis when $K_L > 0$, while it is initially concave to the concentration axis when $K_L < 0$. Since there is often an adsorption heat during a physicochemical adsorption process, the Langmuir or Langmuir-like constants are closely related to the adsorption heat (e.g., the Temkin constant B_1 in the Termkin isotherm model), or the adsorption enthalpy (e.g., the Langmuir constant K_L). Thermal analysis techniques, such as differential scanning calorimetry, are often used to measure the adsorption isotherms.[21,22] The strong evidence through the techniques demonstrates that a set of adsorption isotherms can be represented through the Langmuir or Langmuir-like isotherm constants.

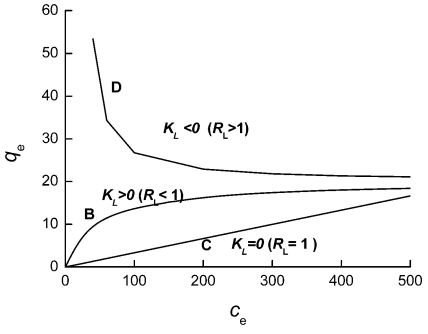

Figure 1. Shapes of the adsorption isotherms indicated with the parameter K_L.

According to eq 2, the shape of Langmuir adsorption isotherm depends on K_L, q_m, and c_e, which could be estimated with the experimental largest equilibrium concentration ($c_{e,m}$). For simplicity, the Langmuir isotherm (eq 2) for ith adsorption system is expressed as L_i (K_{Li}, $c_{e,mi}$, q_{mi}). Therefore, a set of Langmuir adsorption isotherms, L_i (K_{Li}, $c_{e,mi}$, q_{mi}) can easily be transformed into L_i (K_{Li}^N, c_m, q_m^N). q_m^N, the equated maximum adsorption capacity (EMAC), is equal to aq_{mi}, where a denotes the maximum ratio factor of the highest adsorption capacity (q_m^N) to q_{mi}, i.e. ($a = q_m^N/q_{mi}$). Since the maximum adsorption capacity q_m^N is the maximum of q_{mi}, $a \geq 1$. The maximum capacity of all $q_{m\,i}$ for the given set of Langmuir isotherms is selected as q_m^N, which means that all q_{mi} are equal to q_m^N after multiplying the ratio factor a_i . The highest equilibrium concentration c_m is the maximum of all $c_{e,mi}$ and obtained by comparing $c_{e,mi}$ with each other. K_{Li}^N, with a superscript N, means that it is obtained under the conditions of both EMAC and c_m. These adsorption isotherms with EMAC can be expressed as L_1 (K_{L1}^N, c_m, q_m^N), L_2 (K_{L2}^N, c_m, q_m^N), ... L_n (K_{Ln}^N, c_m, q_m^N), respectively. Figures 2 and 3 show the Langmuir adsorption isotherms with EMAC.

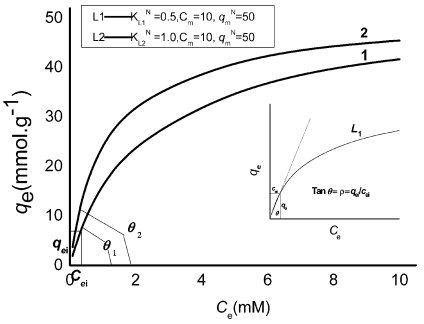

Figure 2. Schematic diagram of the angle θ and comparison of θ_1 and θ_2: curve 1 for L_1 (0.5, 10.0, 50.0) and curve 2 for L_2 (1.0, 10.0, 50.0).

When the concentration $c_e \to 0$, $1 = K_L c_e \to 1$, the isotherm becomes linear (Henry's law):

$$q_e = K_L c_e \text{ or } \frac{q_e}{q_m^N} = K_L^N\left(\frac{c_e}{c_m}\right) \tag{3}$$

The angle between the initial linear part of an isotherm and the concentration axis is denoted as θ, i.e., θ_1 and θ_2 in Figure 2. The magnitude of θ reflects the closeness of an adsorption isotherm to vertical axis in the low sorbate concentration range. However, there is a problem of precise measure of θ, which is known as an unconvenient and error-prone method. Here, a function, tan θ, was introduced to solve the problem. The initial slopes of these isotherm curves (the inset in Figure 2), ρ, are defined as

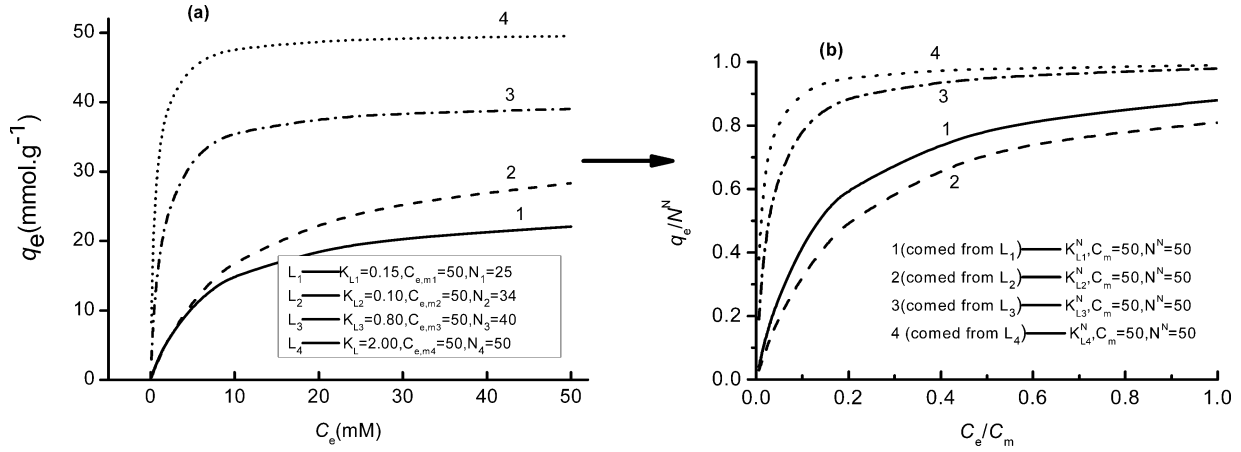

Figure 3. (a) Four different Langmuir adsorption isotherms: curve 1 for L_1 (0.15, 50, 25.0), curve 2 for L_2 (0.1, 50, 34.0), curve 3 for L_3 (0.8, 50, 40.0), curve 4 for L_4 (2.0, 50, 50.0). (b) Four Langmuir adsorption isotherms with EMAA via transformation of original isotherms: curve 1 from L_1 (0.15, 50, 25.0), curve 2 from L_2 (0.1, 50, 34.0), and curve 3 from L_3 (0.8, 50, 40.0).

$$\rho = \tan\theta = \frac{q_e}{c_e} \tag{4}$$

Obviously, $\rho_2 > \rho_1$ is obtained when $\theta_2 > \theta_1$. According to eqs 3 and 4, ρ is related to the magnitude of K_L or K_L^N.

An adsorption isotherm would indicate the adsorbate−adsorbent interaction. Different adsorption mechanisms can be identified with different initial slopes and shapes of the adsorption isotherm curves.[23] For a given set of adsorption isotherms with the different initial slopes, a high slope at a relatively low concentration generally demonstrates a high affinity of the adsorbent surface for the adsorbate.[24] As seen from Figure 2, ρ can be used to characterize the initial slope of an adsorption isotherm, and show the difference of the initial slopes of any two isotherm curves under the condition of $q_{m1}^N = q_{m2}^N$. The larger ρ indicates that the initial part of an adsorption isotherm is closer to the vertical axis (i.e., axis q_e/q_m^N). In Figure 2, the initially linear part of the isotherm L_2 (K_{L2}^N, c_m, q_m^N), which is closer to the vertical axis, shows a larger K_L^N value than the isotherm L_1 (K_{L1}^N, c_m, q_m^N). The transformation of the isotherm L_i (K_{Li}, $c_{e,mi}$, q_{mi}) into the isotherm L_i (K_{Li}^N, c_m, q_m^N) and several adsorption isotherms with different K_L^N values are shown in Figure 3. As shown in Figures 2 and 3, an isotherm with a larger K_L^N clearly gives a higher adsorption capacity at lower concentration. Obviously, K_L^N is related to the initial slope of an adsorption isotherm and can be used to character the initial slope of an adsorption isotherm.

In this paper, a constant separation factor isotherm (eq 7[2,3] or 9) is applied to obtain a dimensionless Langmuir adsorption isotherm with EMAC. Two dimensionless variables (i.e., dimensional concentration[16]), defined elsewhere,[2,3] are introduced:

$$c_e^* = \frac{c_e}{c_{ref}} \tag{5}$$

$$q_e^* = \frac{q_e}{q_{ref}} \tag{6}$$

Here, c_e and c_e^* are the concentration and dimensionless concentration of the adsorbate in liquid phase. q_e and q_e^* are the concentration and the dimensionless concentration of the adsorbate in adsorbed phase. c_{ref} and q_{ref} are the operation concentration in liquid and equilibrium concentration in adsorbed phase.[3] The constant separation factor isotherm is given by[2,3]

$$q_e^* = \frac{c_e^*}{R + (1 - R)c_e^*} \tag{7}$$

where

$$R = \frac{1}{1 + K_L c_{ref}} \tag{8}$$

Equation 9 is obtained by substituting eqs 5−8 into eq 2:

$$\frac{q_e}{q_{ref}} = \left(\frac{c_e}{c_{ref}}\right)\left(\frac{1 + K_L c_{ref}}{1 + K_L c_e}\right) \tag{9}$$

Comparing different expressions of the aforementioned concentrations, i.e., the highest equilibrium concentration c_m (in liquid) and q_m^N (in adsorbed phase), the following relationships were assumed to be reasonable: $c_m \approx c_{ref}$ and $q_m^N \approx q_{ref}$. When $c_m = c_{ref}$ and $q_m^N = q_{ref}$, K_L in eq 9 would be the conditional Langmuir constant K_L^N to comply with the requirement of EMAC. Equation 9 should be

$$\frac{q_e}{q_m^N} = \left(\frac{c_e}{c_m}\right)\left(\frac{1 + K_L^N c_m}{1 + K_L^N c_e}\right) \tag{10}$$

Equation 10 is the dimensionless Langmuir adsorption isotherm with EMAC. Equation 10 is substituted with eq 4 to obtain eq 11a

$$\rho = \frac{1 + K_L^N c_m}{1 + K_L^N c_e} \tag{11a}$$

or eq 11b

$$\rho = \frac{\frac{1}{c_m} + K_L^N}{\frac{1}{c_m} + K_L^N \frac{c_e}{c_m}} \tag{11b}$$

If $(q_e/q_m^N) = 0.4$, for $\rho = 2.0$ ($\theta = 64°$), $(c_e/c_m) = 0.2$ ($c_e = 0.2c_m$). The following equation is obtained from eq 11b:

$$K_L^{N1} = \frac{1}{0.6c_m} \tag{12}$$

dx.doi.org/10.1021/ie401571p | Ind. Eng. Chem. Res. 2013, 52, 14251−14260

If $(q_e/q_m^N) = 0.6$, similarly, $c_e = 0.1c_m$ for $\rho = 6.0$ ($\theta = 80°33'$). Equation 13 is obtained:

$$K_L^{N2} = \frac{5}{0.4c_m} \quad (13)$$

As mentioned before, c_m is invariant for a given set of the adsorption isotherms. Since $(c_e/c_m) < 1$ and $\rho > 1$ when $\theta > 45°$, eq 11b indicates that K_L^N increases with ρ or θ, when θ increases from 45° to 90°. Therefore, the isotherm shapes in the whole range of the Langmuir favorable adsorptions can be predicted through K_L^N or ρ. In other words, the Langmuir favorable adsorption can be evaluated by using the conditional Langmuir constant K_L^N. K_L^N increases faster than ρ with θ (Table 1), which suggests that K_L^N is more sensitive than ρ to evaluate

Table 1. Comparison of ΔK and $\Delta\rho$

θ	ρ	$\Delta\rho$	$K_L^{N\backslash a}$	ΔK_L^N
50°	1.192		0.218	
		0.540		0.667
60°	1.732		0.885	
		0.274		0.366
60°30′	2.006		1.251	
		2.999		6.767
78°42′	5.005		8.018	

$^{\backslash a}$The values were calculated according to eq 10 in the cases assuming $c_e = 0.10$ mM and $c_m = 1.0$ mM.

Langmuir favorable adsorption isotherms in the range $45° < \theta < 90°$. Thereafter, the essential and methodology of the K_L^N method are described to evaluate the Langmuir favorable adsorption.

3. EVALUATION METHODOLOGY

When all the values of R_L are in the range $0 < R_L < 1$, the values of c_m and q_m^N for a given set of Langmuir favorable adsorption isotherms can easily be established with the maximum of $c_{e,mi}$ and of q_{mi}, due to $c_m \geq c_{e,mi}$ and $q_m^N \geq q_{mi}$. Through the assessment of c_m, K_L^{N1}, and K_L^{N1}, the Langmuir favorable adsorptions can be divided meticulously into three subgroups: favorable adsorption, very favorable adsorption, highly favorable or pseudoirreversible adsorption. The above three subgroups are shown with three regions on a dimensionless Langmuir isotherm diagram through two Langmuir isotherms of L_A with the critical Langmuir constants K_L^{N1}, and L_B with K_L^{N2}. The values of K_L^{N1} and K_L^{N2}, at the maximum concentration c_m, can be calculated by using eqs 12 and 13. A part of the critical Langmuir constants are listed in Table 2.

The graphical evaluation for a given Langmuir adsorption isotherm is carried out on a dimensionless Langmuir isotherm diagram to compare two Langmuir isotherms (i.e., lines of demarcation between two zones) curve L_A with K_L^{N1} and curve L_B with K_L^{N2}, respectively (Figure 4).

The initial linear part of each dimensionless Langmuir adsorption isotherm is used to evaluate the favorability. The evaluating criterion of an adsorption isotherm L (K_{L1}^N, $c_{e,mi}$, q_m^N) is illustrated as follows: (I) A favorable adsorption subgroup for the isotherm curve with K_{L1}^N lies in zone I (i.e., K_{L1}^N less than K_L^{N1}). (II) A very favorable adsorption subgroup for the isotherm curve with K_{L1}^N lies in zone II (i.e., K_{L1}^N in the range described by $K_L^{N1} < K_{L1}^N < K_L^{N2}$). (III) A highly favorable or pseudoirreversible adsorption subgroup for the isotherm curve with K_{L1}^N lies in zone III (i.e., K_{L1}^N larger than K_L^{N2}).

Table 2. Critical Values of K_L^N (K_L^{N1} and K_L^{N2}) for the Different Concentration (c_m, mM)

c_m	subgroup I^a	subgroup II	subgroup III^b
0.01	$K_L^N < 166.7$	$166.7 \leq K_L^N \leq 1250$	$K_L^N > 1250$
0.02	$K_L^N < 83.3$	$83.3 \leq K_L^N \leq 625.0$	$K_L^N > 625.0$
0.03	$K_L^N < 55.6$	$55.6 \leq K_L^N \leq 416.7$	$K_L^N > 416.7$
0.05	$K_L^N < 33.3$	$33.3 \leq K_L^N \leq 250.0$	$K_L^N > 250.0$
0.08	$K_L^N < 20.8$	$20.8 \leq K_L^N \leq 156.2$	$K_L^N > 156.2$
0.10	$K_L^N < 16.67$	$16.67 \leq K_L^N \leq 125.0$	$K_L^N > 125.0$
0.20	$K_L^N < 8.33$	$8.33 \leq K_L^N \leq 62.5$	$K_L^N > 62.5$
0.30	$K_L^N < 5.56$	$5.56 \leq K_L^N \leq 41.7$	$K_L^N > 41.7$
0.40	$K_L^N < 4.17$	$4.17 \leq K_L^N \leq 31.25$	$K_L^N > 31.25$
0.50	$K_L^N < 3.33$	$3.33 \leq K_L^N \leq 25.00$	$K_L^N > 25.00$
0.60	$K_L^N < 2.78$	$2.78 \leq K_L^N \leq 20.83$	$K_L^N > 20.83$
0.80	$K_L^N < 2.08$	$2.08 \leq K_L^N \leq 15.63$	$K_L^N > 15.63$
0.90	$K_L^N < 1.85$	$1.85 \leq K_L^N \leq 13.89$	$K_L^N > 13.89$
1.00	$K_L^N < 1.67$	$1.67 \leq K_L^N \leq 12.50$	$K_L^N > 12.50$
3.00	$K_L^N < 0.56$	$0.56 \leq K_L^N \leq 4.17$	$K_L^N > 4.17$
5.00	$K_L^N < 0.33$	$0.33 \leq K_L^N \leq 2.50$	$K_L^N > 2.50$
10.0	$K_L^N < 0.167$	$0.167 \leq K_L^N \leq 1.25$	$K_L^N > 1.25$
50.0	$K_L^N < 0.033$	$0.033 \leq K_L^N \leq 0.25$	$K_L^N > 0.25$
100.0	$K_L^N < 0.017$	$0.017 \leq K_L^N \leq 0.125$	$K_L^N > 0.125$

$^a K_L^N < K_L^{N1}$, the values of K_L^{N1} can be calculated with eq 12. $^b K_L^N > K_L^{N2}$, the values of K_L^{N2} can be calculated with eq 13.

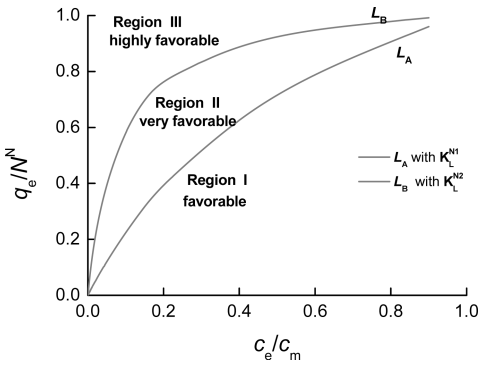

Figure 4. Three regions on a dimensionless Langmuir adsorption isotherm through the graphical K_L^N method: $c_m = 50$ mM, $K_L^{N1} = 0.033$ L (mmol)$^{-1}$, $K_L^{N2} = 0.25$ L (mmol)$^{-1}$.

To evaluate the favorability of isotherm L_1 (K_{L1}, $c_{e,mi}$, q_{m1}) ($L1$) through the K_L^N method, the general procedures are as follows: (i) K_{L1} and q_{m1} for the isotherms L_1 are conventionally obtained by analyzing the adsorption equilibrium data through a linear regression equation (eq 15) or nonlinear equation (eq 2). (ii) a_i values are determined through $a_i = q_m^N/q_{mi}$. c_m is set to be the maximum c_{ei} and the critical Langmuir constants, K_L^{N1} and K_L^{N2}, at c_m were established from Table 2. The dimensionless isotherms L_A (K_L^{N1}, c_m, q_m^N), L_B (K_L^{N2}, c_m, q_m^N) and L_2 (K_{L2}^N, c_m, q_m^N) (L_2), resulted from L_1, are plotted on a dimensionless Langmuir isotherm diagram. (iii) The favorability of adsorption isotherm L_2, namely the favorability of L_1, is evaluated through the location of the initial part of L_2 on the dimensionless Langmuir isotherm diagram.

4. EXPERIMENTAL SECTION

4.1. Synthesis of Propr-IP Adsorbents. Propranolol-imprinted polymer (Propr-IP) is synthesized through a noncovalent method as previously described.[25] Three kinds of porogen solvent, methanol (MeOH), chloroform, and toluene,

dx.doi.org/10.1021/ie401571p | Ind. Eng. Chem. Res. 2013, 52, 14251−14260

are used to prepare the polymers. The template (Propr), functional monomer (MMA), cross-linker (TMP), and the initiator (AIBN) are mixed with the molar ratio Propr/MMA/TMP = 1:4:4, with the porogen in a glass flask. The solution is then stirred and purged with nitrogen for 10 min. The flask is sealed under nitrogen. The polymerization takes place in water bath at 65 °C for 24 h. The resulting polymer is milled and sieved, yielding particles with diameters of 20−34 μm. The template in the remaining particles is removed successively with MeOH/acetic acid (8:2, v/v), MeOH, and water. The potential response of the collected aqueous solution is determined by using Propranolol ion-selective electrode.[26] The potential response of the aqueous solution is close to that of the blank solution, and the concentration of Propr·HCl is less than 3.0×10^{-6} M.

The polymer particles are dried at 55 °C under vacuum. Adsorbents A, B, and C are named for the Propr-IPs prepared from different solvents of MeOH, chloroform, and toluene, respectively.

4.2. Study of Batch Adsorption. A 20 mg portion of polymer is placed in a set of 50-mL iodine flasks. A set of 10 Propr·HCl aqueous solutions of 3.0×10^{-5} to 10.0×10^{-6} M is prepared. An aliquot of 10.0 mL of each solution is added into the iodine flask and stopped. The mixture is shaken with a HY-4 speed controlled bed shaker (Shanghai, China) for 10 h at 25 °C and then centrifuged. Both the supernatant and its original solution are analyzed to determine Propr·HCl through the potentiometric method, as described before. The adsorption capacity of bound compound is calculated by using the following equation:

$$q_e = \frac{(c_0 - c_e)V}{m} \tag{14}$$

Here, c_o (mM) is the initial concentration, c_e (mM) is the concentration of final supernatant, m (g) is the mass of adsorbent, V (L) is the volume of the solution, and q_e is the adsorption capacity (mmol g^{-1}). Each adsorption analysis is repeated three times, and the average value is adopted. The experimental equilibrium data are analyzed by using the linear form of the Langmuir isotherm equation:

$$\frac{c_e}{q_e} = \frac{1}{K_L q_m} + \frac{c_e}{q_m} \tag{15}$$

q_m (mmol g^{-1}) and K_L (L $mmol^{-1}$) were computed from the slope and intercept of the linear plot of c_e/q_e versus c_e.

The equilibrium data are also analyzed by using the linear form of the Freundlich isotherm, which can be described as

$$\log q_e = \left(\frac{1}{n_F}\right)\log c_e + \log K_F \tag{16}$$

where K_F [$(mmol)^{1-1/n_F}L^{1/n_F}\,g^{-1}$] is the Freundlich constant and n_F is an empirical constant. K_F and n_F are obtained from the intercept and slope of the plots of log q_e versus log c_e, respectively.

5. RESULTS AND DISCUSSION

5.1. K_L^N and Selections of c_m, N^N, and a. When ρ ($\rho \neq 1$) is constant, and eq 11a is rearranged as follows

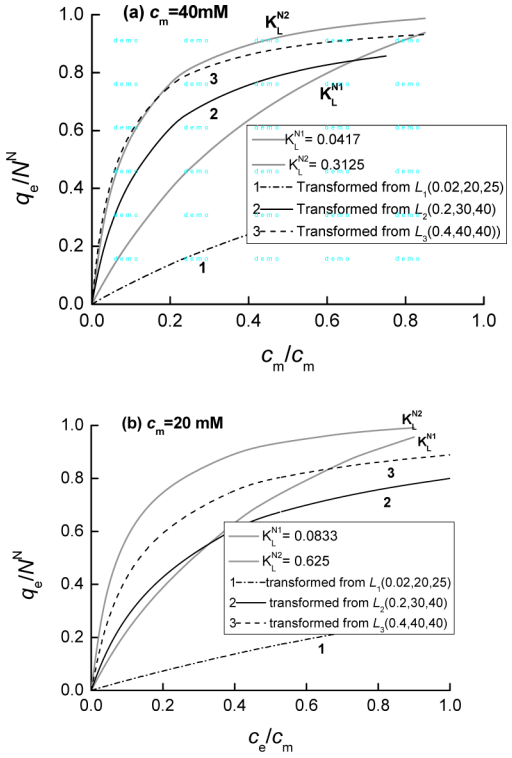

Figure 5. Effect of c_m on the shape of adsorption isotherms. Three transformed adsorption isotherms with EMAA (N^N = 50 mmol g^{-1}) are curve 1 from L_1 (0.02, 20, 25.0), curve 2 from L_2 (0.2, 30, 40.0), and curve 3 from L_3 (0.4, 40, 40.0), respectively. (a) c_m = 40 mM; (b) c_m = 20 mM.

$$K_L^N = \frac{\rho - 1}{c_m\left(1 - \left(\frac{c_e}{c_m}\right)\rho\right)} \tag{17}$$

According to eq 17, the Langmuir constant K_L^N varied with different c_m and different ρ.

If $\rho > 1$, $K_L^N > 0$, and the adsorption isotherm should be convex. If $\rho < 1$, K_L^N is less than zero, and the adsorption isotherm would be concave, due to $c_m > 0$ and $c_e > 0$. If $\rho = 1$, K_L^N is zero, and the Langmuir adsorption isotherm would be a straight line with the angle between the line and the concentration axis (θ) of 45°. So, the Langmuir constant K_L^N can also be applied to characterize different types of Langmuir isotherms graphically with the same efficiency as the R_L parameter.

The highest equilibrium concentration c_m is first selected through the K_L^N method. If c_m is set to be too small, e.g., smaller than $c_m/2$, relative flat curves for the adsorption isotherms would be plotted and the classification of the favorability subgroup would be inaccurate. Figure 5 shows the effect of c_m on the value of K_L^N and the shapes of adsorption isotherms. The value of K_L^N for the isotherm curve 3 is larger than the K_L^{N2} when c_m = 40 mM (Figure 5a), while it falls between K_L^{N1} and K_L^{N2} when c_m = 20 mM (Figure 5b).

To study the effect of q_m^N on the shapes of Langmuir adsorption isotherms, a general Langmuir adsorption isotherm L (K_{Li}, c_m, q_{mi}) is transformed into two different isotherms, L_1 and L_2, with different maximum adsorption capacities.

Let L_1 to be L (K_L^{N1}, c_m, q_m^{N1}), L_2 to be L (K_L^{N2}, c_m, q_m^{N2}), $((q_m^{N1})/(q_{mi})) = a_1$, and $((q_m^{N2})/(q_{mi})) = a_2$, and then the fractions of adsorption capacities of isotherms are $((a_1 q_e)/$

dx.doi.org/10.1021/ie401571p | Ind. Eng. Chem. Res. 2013, 52, 14251−14260

Table 3. Langmuir and Freundlich Constants for the Adsorption of Propr·HCl onto MIPs

	Langmuir model				Freundlich model		
adsorbent	q_m (mmol g^{-1})	K_L (L mmol^{-1})	r	R_L[a]	K_F	n_F	r
MIP(A)	0.0356 ± 0.0066	34.38 ± 2.78	0.9864	0.267	0.119 ± 0.006	1.841 ± 0.037	0.9725
MIP(B)	0.0341 ± 0.0011	21.69 ± 2.19	0.9322	0.366	0.158 ± 0.016	1.369 ± 0.064	0.9316
MIP(C)	0.0284 ± 0.0013	13.57 ± 1.71	0.9530	0.496	0.153 ± 0.013	1.133 ± 0.050	0.9320

[a] c_0 = 0.080 mM.

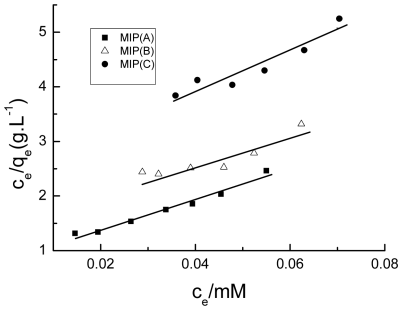

Figure 6. Langmuir plots for adsorption of Propr·HCl on three MIP adsorbents.

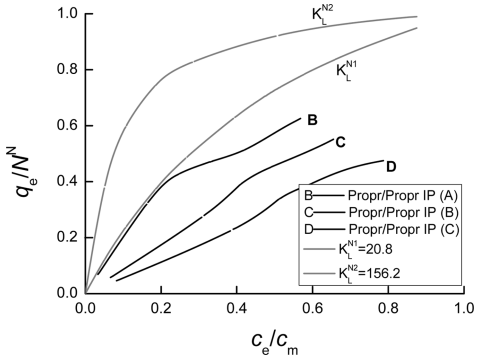

Figure 7. Favorable evaluation of three Propr·HCl/Propr-MIP adsorption systems by using the K_L^N method. q_m^N = 0.05 mmol g^{-1}, c_m = 0.080 mM.

$(q_m^{N1}))$ for L_1 and $((a_2q_e)/(q_m^{N2}))$ for L_2 at the concentration c_e, respectively. The following stoichiometric relation would be held:

$$\frac{a_1 \cdot q_e}{q_m^{N1}} = \frac{q_e}{q_{mi}} = \frac{a_2 \cdot q_e}{q_m^{N2}}$$

This indicates that q_m^N does not affect the shape of a Langmuir adsorption isotherm. In other words, the selection of q_m^N does not affect K_L^N of the Langmuir isotherms with EMAC (K_L^{N1} = K_L^{N2}). According to eqs 11 and 17, it is also confirmed that the magnitude of K_L^N is independent of q_m^N. K_L^N is also not affected by the selection of a, since q_m^N does not affect K_L^N of Langmuir isotherms. The maximum ratio factor (a) is generally between 1 and 2.

5.2. Application of K_L^N Method. *A. Propr/Propr-IP Adsorption Systems.* The Langmuir adsorption isotherm is an ideal adsorption model, which assumes monolayer adsorption of adsorbate on a homogeneous adsorbent surface with finite identical sites, which are energetically equivalent, and the interactions among the adsorbed molecules are negligible. In some real adsorptions reported in literature, the interactions of the molecules are not zero, and the adsorbate has an intermolecular attraction to the surface of the adsorbent. Since in most cases these interactions are not strong, the Langmuir isotherms can still be applied in these cases.

The experimental sorption data of three Propr-IP adsorbents are analyzed through both Langmuir isotherm model and Freundlich isotherm model. The Langmuir constants (q_{mi} and K_L) are determined by using eq 15. K_F and n_F are determined through the intercepts and the slopes of the plots of log q_e

Table 4. Comparison of K_L^N Method with R_L and n_F Methods for Favorable Evaluation

	K_L^N method		R_L method			n_F method		
adsorption system	subgroup	evaluation	c_0 (mg L^{-1})	R_L (inlit)	evaluation	n_F (inlit)	evaluation	ref
AR151/CDBA-hectorite	III	highly favorable	(264.6)[a]	0.005	favorable	12.30	?	28
AR151/CP-hectorite	III	highly favorable	(223)[a]	0.0071	favorable	9.75	favorable	28
DB2B/AC prepared from sawdust	III	highly favorable	(404)[a]	0.03	favorable	5.03	favorable	27
AR/treated carbon (600 °C)	III	highly favorable	(248)[a]	0.083	favorable	n_{F1}:1.90 n_{F2}:5.80	favorable ?	31
MB/PAC2 (pH = 11)	III	highly favorable	(484)[a]	0.007	favorable	6.43	favorable	29
MB/Florisil (*dp*112)	III	highly favorable	500	0.021	favorable	11.26	?	10
			2000	0.005	favorable			
MB/crushed brick	II	very favorable	(40)[a]	0.0237	favorable	2.83	favorable	11
BR22/palm- fruit bunch	II	very favorable	(152.3)[a]	0.023	favorable	n_{F1}:1.91 n_{F2}:8.17	favorable ?	30
AR97/AC	II	very favorable	(30)[a]	0.23	favorable	2.99	favorable	32
Pb^{2+}/Chitosan	I	favorable	(0.50 mM)	(0.368)[b]	favorable	0.58[c]	?	33
TCP/coconut husk-based AC	I	favorable	25	0.734	favorable	1.20[c]	favorable	34
Propr·HCl/Propr-IP(A)	I	favorable	0.080 (mM)	0.267	favorable	1.84	favorable	this work
Propr·HCl/Propr-IP(B)	I	favorable	0.080 (mM)	0.366	favorable	1.31	favorable	this work
Propr·HCl/Propr-IP(C)	I	favorable	0.080 (mM)	0.496	favorable	1.13	favorable	this work

[a] The values of c_0 in parentheses were obtained from the values of R_L reported in literature by using eq 1. [b] The estimated value of R_L is 0.368 by taking c_0 = 0.50 mM. [c] The values of n_F, 0.58 and 1.20, were obtained from the values $1/n_F$ = 1.721 and $1/n_F$ = 0.83, respectively.

dx.doi.org/10.1021/ie401571p | Ind. Eng. Chem. Res. 2013, 52, 14251−14260

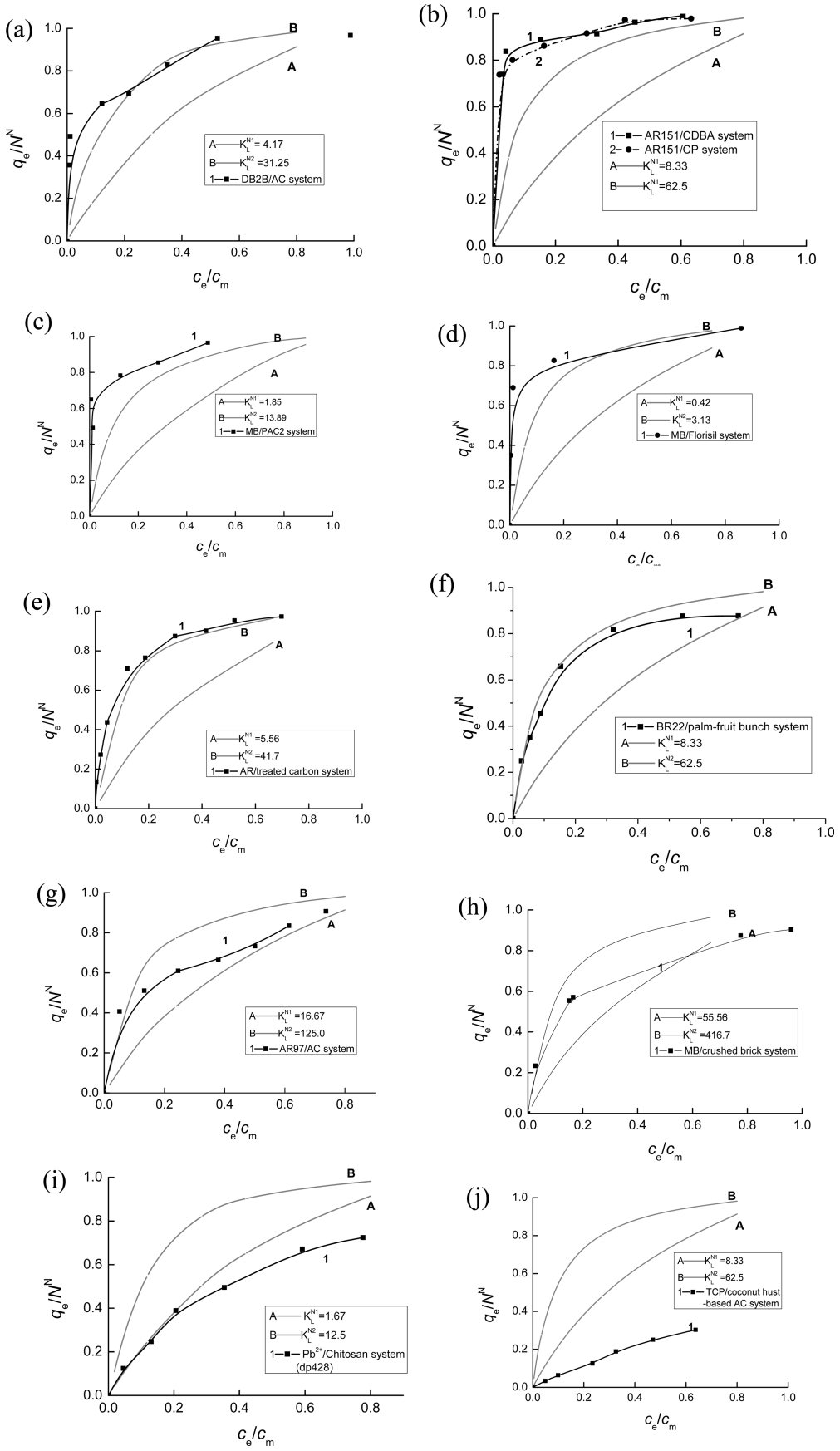

Figure 8. Graphical evaluation of K_L^N method for 11 different adsorption systems. (a) Adsorption isotherm (curve 1) for DB2B/AC from sawdust adsorption system: q_m^N = 0.700 mmol g^{-1}, c_m = 0.40 mM, a = 1.083. (b) Adsorption isotherm: curve 1 (■) (a_1 = 1.435) for AR151/CDBA-hectorite system; curve 2 (●) (a_2 = 1.742) for AR151/CP-hectorite system. q_m^N = 0.700 mmol g^{-1}, c_m = 0.20 mM. (c) Adsorption isotherm (curve 1) for MB/

dx.doi.org/10.1021/ie401571p | Ind. Eng. Chem. Res. 2013, 52, 14251−14260

Figure 8. continued

PAC2 adsorption system: q_m^N = 3.00 mmol g^{-1}, c_m = 1.0 mM, a = 1.367. (d) Adsorption isotherm (curve 1) for MB/Florisil (dp112) adsorption system: q_m^N = 0.500 mmol g^{-1}, c_m = 4.0 mM, a = 1.128. (e) Adsorption isotherm (curve 1) for AR/treated carbon (600 °C) adsorption system: q_m^N = 0.300 mmol g^{-1}, c_m = 0.30 mM, a = 1.141. (f) Adsorption isotherm (curve 1) for BR22/palm-fruit bunch system: q_m^N = 0.700 mmol g^{-1}, c_m = 0.20 mM, a = 1.008. (g) Adsorption isotherm (curve 1) for AR97/AC adsorption system: q_m^N = 0.100 mmol g^{-1}, c_m = 0.10 mM, a = 1.326. (h) Adsorption isotherm (curve 1) for MB/crushed brick adsorption system: q_m^N = 0.400 mmol g^{-1}, c_m = 0.03 mM, a = 1.185. (i) Adsorption isotherm (curve 1) for Pb^{2+}/chitosan adsorption system: q_m^N = 0.300 mmol g^{-1}, c_m = 1.0 mM, a = 1.007. (j) Adsorption isotherm (curve 1) for TCP/coconut adsorption system: q_m^N = 4.000 mmol g^{-1}, c_m = 0.20 mM, a = 1.188.

versus log c_e (eq 16). The results including the regression coefficient (R) are listed in Table 3. Figure 6 shows the Langmuir plots of Propr·HCl adsorption on three Propr-IP adsorbents. The linear fitting result through the Langmuir model was better than that through the Freundlich model. In addition, the results of $1/n_F < 1$ from the Freundlich model also indicate that the adsorptions obey the Langmuir isotherm. The good fitting result through the Langmuir model suggested that Propr·HCl-IP forms a monolayer coverage on the adsorbent surfaces. Figure 7 shows the dimensionless Langmuir adsorption isotherms and two critical Langmuir isotherms with K_L^{N1} and K_L^{N2}. Clearly, three adsorption isotherms (B, C, and D) belong to favorable adsorption subgroup. While there is a large variation of R_L, e.g., for isotherm B for Propr·HCl/Propr-IP(A) adsorption system, ranging from 0.0072 (c_0 = 4 mM) to 0.267 (c_0 = 0.08 mM), values depend on the magnitude of c_0. Obviously, the K_L^N method is more objective than the R_L method, whose result is heavily affected by the initial concentrations.

B. Application of K_L^N Method to the Adsorption Systems in Literature. The 11 liquid−solid adsorption systems previously reported in literature are chosen as follows: Direct Blue 2B/activated carbon prepared from sawdust carbon (DB2B/AC prepared from sawdust),[27] Acid Red 151/modified cetyldimethylbenzylammonium chloride-hectorite (AR151/CDBA-hectorite) and Acid Red 151/cetylpyridinium chloride-hectorite (AR151/CP-hectorite),[28] MB/activated carbon (PAC2) (pH = 11),[29] Basic Red (BR22)/palm-fruit bunch,[30] MB/magnesium silicate (Florisil) (dp 112),[10] Acid Red 73(AR)/treated carbon (600 °C),[31] Acid Red 97/activated carbon (AR97/AC),[32] Pb^{2+}/Chitosan (dp 428 and pH = 4.50),[33] 2,4,6-trichlorophenol/coconut husk-based activated carbon (TCP/coconut husk-based AC),[34] and MB/crushed brick.[11] All of them obey Langmuir adsorption isotherm. The Langmuir constants (K_L and q_{mi}) or parameters (R_L and n_F) in Table S1 are from the literature. All adsorption systems in Table 4, except the Pb^{2+}/Chitosan system, clearly belong to favorable adsorption if separation factor (R_L) is the only criterion.

The experimental data of the equilibrium isotherm graphs are reproduced and reanalyzed through eq 15. The results including the regression coefficient (R) are listed in Table S1 .The reanalyzed Langmuir constants (q_{mi} and K_L) are very close to those reported in literature. The graphical evaluations of Langmuir favorable adsorption for the 11 adsorption systems are shown in Figure 8. On the basis of the graphical K_L^N method (Table 4), six Langmuir adsorption systems, DB2B/AC prepared from sawdust, AR/CDBA-hectorite, AR/CP-hectorite, MB/florisil (dp112), AR/treated carbon (600 °C), and MB/PAC2, are obviously highly favorable adsorption. Two adsorption systems, TCP on coconut and Pb^{2+}/Chitosan, belong to favorable adsorption. Three other adsorption systems, MB/crushed brick, BR22/palm-fruit bunch, and AR97/AC, belong to very favorable adsorption, although R_L of Pb^{2+}/Chitosan adsorption system was not provided in the literature. Obviously, as compared with the R_L method, the graphical K_L^N method has the following advantages: (1) The parameter K_L^N does not depend on the initial adsorbate concentration (c_o), while R_L does. (2) For the favorable evaluation ($0 < R_L < 1$), there are three subgroups of favorable adsorption in the K_L^N method to be used to further distinguish the favorability. (3) The graphical $K_L{}^N$ method is intuitive because of the application of the dimensionless Langmuir adsorption isotherm diagram.

C. Comparison of the K_L^N Method to the n_F Method. The n_F values of Propr·HCl/Propr-IPs, AR151/CDBA-hectorite, and so forth adsorption systems are listed in Table 4. Since the n_F values of AR/treated carbon (600 °C) and MB/Florisil (dp112) are not reported in the literature, they are obtained by reanalyzing the experimental data on the isotherm graphs. According to the K_L^N method, six adsorption systems (in Table 4), AR151/CDBA-hectorite, AR151/CP-hectorite, DB2B/AC, AR/treated carbon (600 °C), MB/PAC2 (pH = 11), and MB/Florisil (dp112), belong to the highly favorable. On the other hand, the n_F of the following systems, i.e., AR/CDBA-hectorite (12.3), MB/Florisil (dp112) (11.26), are larger than 10.0. On the basis of the n_F method, obviously, these adsorptions cannot be classified as favorable adsorption. Two n_F values (1.91, 8.17) of BR22/palm-fruit bunch system are obtained from the equilibrium isotherm graph,[30] since the plot of log q_e versus log c_e shows two slopes in two parts. Two n_F values of the AR/treated carbon (600 °C) isotherm system also are shown in Table 4. In these cases, since the n_F method may cause the ambiguity for the favorable evaluation, it is not appropriate to evaluate the adsorption favorability through the n_F method. The graphical K_L^N method can used to evaluate any Langmuir favorable adsorption. Another advantage of the K_L^N method is intuititiveness, and the parameter K_L^N has a certain physical meaning. Therefore, the mathematical model of the K_L^N method for the favorable evaluation is superior to those of the R_L method and the n_F method.

6. CONCLUSIONS

This work proposed a graphical method for evaluating the Langmuir favorable adsorption behavior based on the use of the conditional Langmuir constant (K_L^N) and the dimensionless Langmuir adsorption isotherm. All the Langmuir favorable adsorptions (i.e., $0 < R_L < 1.0$) can be classified into three subgroups: favorable adsorption subgroup, very favorable adsorption subgroup, and highly favorable or pseudoirreversible adsorption subgroup, through the critical values of K_L^N, K_L^{N1} and K_L^{N2} at the highest concentration (c_m). The graphical K_L^N method has been successfully applied to evaluate the Langmuir favorable adsorption for 14 different adsorption systems. The method is more objective and simpler, and shows better comparison than the present R_L and n_F method to evaluate Langmuir favorable adsorption of different systems.

■ ASSOCIATED CONTENT

Supporting Information

Table of data for the experimental Langmuir constant (q_m, K_L) and the values for R_L and n_F for 11 different adsorption systems reported in literature, and values for the reanalyzed Langmuir constant (q_m, K_L) through reanalyzing the reported adsorption isotherms and the regression coefficient (R). This material is available free of charge via the Internet at http://pubs.acs.org.

■ AUTHOR INFORMATION

Corresponding Author

*E-mail: lingzhi.sun@yahoo.cn. Fax:+86-0519-86330167.

Notes

The authors declare no competing financial interest.

■ ACKNOWLEDGMENTS

C.-J.S. gratefully acknowledges funding from Zhejiang Science and Technology Innovations Team Project Grant 2010R50012, the Research Keystone Programs of Jiaxing University 70112024BL, and the Research Start-Up Program of Jiaxing University 70512002. This work was supported by the Scientific Reseach Startup Fund 6212126034 from Yancheng Teachers University.

■ SYMBOLS USED

a, a_i (−) = maximum capacity factor: $a = (q_m^N)/(q_{mi})$
$B1$ (−) = Temkin constant in the Temkin isotherm model
c_e, $c_{e,mi}$ (mM) = equilibrium concentration (or liquid-phase concentration of the adsorbate) and the experimental highest equilibrium concentration (or the experimental maximum liquid-phase concentration of the adsorbate)
c_{ref} (mM) = operation concentration
c_m (mM) = the calculating highest equilibrium concentration (or calculating highest liquid-phase concentration of the adsorbate)
c_o (mM) = (experimental) initial concentration
EMAC (−) = equal maximum adsorption capacity (i.e., the case of q_m^N used)
K_F (mmol$^{1-1/n}$L$^{1/n}$ g^{-1}) = Freundlich constant
K_L, $K_{L,i}$ [L (mmol)$^{-1}$] = Langmuir constant
K_L^N, K_L^{Ni} [L (mmol)$^{-1}$] = conditional Langmuir constant
ΔK_L^N [L (mmol)$^{-1}$] = increment of conditional Langmuir constant
L_1, L_A (−) = Langmuir adsorption isotherm or isotherm function
m (g) = mass of adsorbent
n_F (−) = dimensionless Freundlich constant
q_m, q_{mi} (mmol g^{-1}) = experimental maximum adsorption capacity (or experimental maximum adsorbed-phase concentration of the adsorbate)
q_m^N (mmol g^{-1}) = equal, calculating maximum adsorption capacity (or calculating maximum adsorbed-phase concentration of the adsorbate)
q_c, q_e, q_{ei}' (mmol g^{-1}) = equilibrium adsorption capacity (or adsorbed-phase concentration of the adsorbate)
q_{ref} (mmol g^{-1}) = adsorbed-phase concentration in equilibrium with the concentration c_{ref}
R_L (—) = dimensionless separation factor
V (L) = volume of solution

Greek Letters

θ (deg) angle between lines
ρ (−) parameter, $\rho = \tan\theta$
$\Delta\rho$ (−) increment of tan θ

■ REFERENCES

(1) Frank, L. S. *Adsorption Technology: A Step by Step Approach to Process Evaluation and Application*; Dekker: New York,1985.
(2) LeVan, M. D. Pressure Swing Adsorption: Equilibrium Theory for Purification and Enrichment. *Ind. Eng. Chem. Res.* **1995**, *34*, 2655.
(3) Owens, D. J.; Ebner, A. D.; Ritter, J. A. Equilibrium Theory Analysis of a Pressure Swing Adsorption Cycle Utilizing a Favorable Langmuir Isotherm: Approach to Periodic Behavior. *Ind. Eng. Chem. Res.* **2012**, *51*, 13454.
(4) Mazzotti, M.; Tarafder, A. A Method for Deriving Explicit Binary Isotherms Obeying the Ideal Adsorbed Solution Theory. *Chem. Eng. Technol.* **2012**, *35*, 102.
(5) Thompson, G.; Swain, J.; Kay, M.; Forster, C. F. The Treatment of Pulp and Paper Mill Effluent: A Review. *Bioresour. Technol.* **2001**, *77*, 275.
(6) Langmuir, I. The Adsorption of Gases on Plane Surfaces of Glass, Mica, and Platinum. *J. Am. Chem. Soc.* **1918**, *40*, 1361.
(7) Moradi, O.; Aghaie, M.; Zare, K.; Monajjemi, M.; Aghaie, H. The Study of Adsorption Characteristics Cu^{2+} and Pb^{2+} Ions onto PHEMA and P(MMA-HEMA) Surfaces from Aqueous Single Solution. *J. Hazard. Mater.* **2009**, *170*, 673.
(8) Liu, Y.; Liu, Y.-J. Biosorption Isotherms, Kinetics and Thermodynamics. *Sep. Purif. Technol.* **2008**, *61*, 229.
(9) Eren, Z.; Acar, F. N. Adsorption of Reactive Black 5 from An Aqueous Solution: Equilibrium and Kinetic Studies. *Desalination* **2006**, *194*, 1.
(10) Ferrero, F. Adsorption of Methylene Blue on Magnesium Silicate: Kinetics, Equilibia and Comparison with Other Adsorbents. *J. Environ. Sci.* **2010**, *22*, 467.
(11) Hamdaoui, O. Batch Study of Liquid-Phase Adsorption of Methylene Blue Using Cedar Sawdust and Crushed Brick. *J. Hazard. Mater.* **2006**, *B135*, 264.
(12) Moradi, O.; Fakhri, A.; Adami, S.; Adami, S. Isotherm, Thermodynamic, Kinetics, and Adsorption Mechanism Studies of Ethidium Bromide by Single-Walled Carbon Nanotube and Carboxylate Group Functionalized Single-Walled Carbon Nanotube. *J. Colloid Interface Sci.* **2013**, *395*, 224.
(13) Moradi, O.; Zare, K. Adsorption of Pb(II), Cd(II) and Cu(II) Ions in Aqueous Solution on SWCNTs and SWCNT−COOH Surfaces: Kinetics Studies. *Fullerenes, Nanotubes, Carbon Nanostruct.* **2011**, *19*, 628.
(14) Najafi, F. Investigation of a QM/MM Study on Interaction of a Carbon Nanotube with Cytarabine Drug in Various Solvents and Temperatures. *J. Nanostruct. Chem.* **2013**, *3*, 23.
(15) Ayad, M. M.; El-Nasr, A. A. Anionic Dye (Acid Green 25) Adsorption from Water by Using Polyaniline Nanotubes Salt/Silica Composite. *J. Nanostruct. Chem.* **2012**, *3*, 3.
(16) Hall, K. R.; Eagleton, L. C.; Acrivos, A.; Vermeulen, T. Pore-and Solid-Diffusion Kinetics in Fixed-Bed Adsorption under Constant-Pattern Conditions. *Ind. Eng. Chem. Fundamen.* **1966**, *5*, 212.
(17) Freundlich, H. M. F. Over the Adsorption in Solution. *J. Phys. Chem.* **1906**, *57*, 385.
(18) Tseng, R. L.; Wu, F. C. Analyzing Concurrent Multi-Stage Adsorption Process of Activated Carbon with A Favorable Parameter of Langmuir Equation. *J. Taiwan Inst. Chem. Eng.* **2009**, *40*, 197.
(19) Konaganti, V. K.; Kota, R.; Patil, S.; Madras, G. Adsorption of Anionic Dyes on Chitosan Grafted Poly(alkyl methacrylate)s. *Chem. Eng. J.* **2010**, *158*, 393.
(20) Weber, T. W.; Chakravorti, R. K. Pore and Solid Diffusion Models for Fixed-Bed Adsorbers. *AIChE J.* **1974**, *20*, 228.
(21) Eusebio, L.; Fumagalli, D.; Gronchi, P. Thermal Evidences of the Interaction between Plasticizers and Ca Salts in Cement. *J. Therm. Anal. Calorim.* **2009**, *97* (1), 33.
(22) McFarlane, N. L.; Wagner, N. J.; Kaler, E. W.; Lynch, M. L. Calorimetric Study of the Adsorption of Poly(ethylene oxide) and Poly(vinyl pyrrolidone) onto Cationic Nanoparticles. *Langmuir* **2010**, *26*, 6262.

(23) Lawrence, M. A. M.; Davies, N. A.; Edwards, P. A.; Taylor, M. G.; Simkiss, K. Can Adsorption Isotherms Predict Sediment Bioavailability? *Chemosphere* **2000**, *41*, 1091.
(24) Hubbe, M. A.; Wu, N.; Rojas, O. J.; Park, S. Permeation of A Cationic Polyelectrolyte into Mesoporous Silica Part 3. Using Adsorption Isotherms to Elucidate Streaming Potential Results. *Colloids Surf., A* **2011**, *381*, 1.
(25) Sun, X.; Qiu, Y.; Xie, A.; Wang, Z.; Su, Z. Synthetic Receptor for Propranolol-Synthesis and Molecular Recognition of Molecular Iimprinted Polymer. *Jiangsu Gongye Xueyuan Xuebao* **2008**, *20* (3), 50.
(26) Aboul-Enein, H. Y.; Sun, X. X. A Novel Ion Selective PVC Membrane Electrode for Determination of Propranolol in Pharmaceutical Formulation. *Analusis* **2000**, *28*, 855.
(27) Malik, P. K. Dye Removal from Wastewater Using Activated Carbon Developed from Sawdust: Adsorption Equilibrium and Kinetics. *J. Hazard. Mater.* **2004**, *B113*, 81.
(28) Baskaralingam, P.; Pulikesi, M.; Ramamurthi, V.; Sivanesan, S. Equilibrium Studies for the Adsorption of Acid Dye onto Modified Hectorite. *J. Hazard Mater.* **2006**, *B136*, 989.
(29) El Qada, E. N.; Allen, S. J.; Walker, G. M. Adsorption of Methylene Blue onto Activated Carbon Produced from Steam Activated Bituminous Coal: A Study of Equilibrium Adsorption Isotherm. *Chem. Eng. J.* **2006**, *124*, 103.
(30) Nassar, M. M.; Magdy, Y. H. Removal of Different Basic Dyes from Aqueous Solutions by Adsorption on Palm-Fruit Bunch Particles. *Chem. Eng. J.* **1997**, *66*, 223.
(31) Attia, A. A.; Rashwan, W. E.; Khedr, S. A. Capacity of Activated Carbon in the Removal of Acid Dyes Subsequent to Its Thermal Treatment. *Dyes Pigm.* **2006**, *69*, 128.
(32) Gomez, V.; Larrechi, M. S.; Callao, M. P. Kinetic and Adsorption Study of Acid Dye Removal Using Activated Carbon. *Chemosphere* **2007**, *69*, 1151.
(33) Ng, J. C. Y.; Cheung, W. H.; McKay, G. Equilibrium Studies for the Sorption of Lead from Effluents Using Chitosan. *Chemosphere* **2003**, *52*, 1021.
(34) Hameed, B. H.; Tan, I. A. W.; Ahmad, A. L. Adsorption Isotherm,Kinetic Modeling and Mechanism of 2,4,6-Trichlorophenol on Coconut Husk-Based Activated Carbon. *Chem. Eng. J.* **2008**, *144*, 235.